# Observations of mesospheric gravity wave dynamics in the southern hemisphere

Jonathan Pugmire, Mike Taylor
Utah State University

**Abstract- Observations of mesospheric OH rotational temperature by the Mesospheric Temperature Mapper located at Cerro Pachon, Chile (30.3°S, 70.7°S) show a large range of variation. Temperature variances reveal increased activity due to mountain waves. Comparative studies with the satellite carried SABER instrument show agreement on nightly, as well as seasonal, temperature measurements. Comparisons with similar temperature measurements from Maui, Hawaii (20.8°N) reveal mountain wave activity to be enhanced over the Andes in the winter months. Initial gravity wave measurements from McMurdo Base, Antarctica are highlighted.**

## 1. INTRODUCTION

The Andes Mountain Range in South America is an excellent natural laboratory for investigating the effects of atmospheric gravity waves (AGW) on the upper atmospheric wind and temperature fields. AGW propagate freely throughout the atmosphere transporting large amounts of momentum and energy from near the Earth's surface to great altitudes where they dissipate. AGW are arguably the most important process coupling all altitudes of the neutral atmosphere (0-100 km altitudes) [Fritts and Alexander, 2003]. The mesosphere and lower-thermosphere (MLT) region (60-100 km) is a key region to study and to understand these coupling mechanisms. The Andes region in South America is of particular interest because during the winter strong mountain forcing is expected to dominate in the creation of AGW due to intense prevailing winds blowing eastward from the Pacific Ocean that suddenly encounter the towering Andes mountain range (average height 4000 m).

Large amplitude mountain waves (lee waves) have been measured penetrating into the stratosphere above a number of prominent mountain ranges [Eckerman and Preusse, 1999] but their effects have yet to be quantified in the mesosphere [Smith et al., 2009]. Mountain waves are characterized by having a zero horizontal phase speed as observed from the ground. This is because they are generated by strong winds blowing over prominent mountains and so their phase speeds are equal to and in the opposite direction of the wind which is perpendicular to the mountain range. Mountain waves are prominent in the winter months because they

**Figure 1**. The Andes LIDAR Observatory located in the Andes Mountains near the Cerro Pachon astronomical observatory in Chile.

**Figure 2**. Picture of all-sky imaging system. Fish eye lens at top, followed by filter wheel. CCD imager and cooling system are positioned at bottom.

are not filtered out by critical layer wind filtering. A critical layer is when the wind speed is equal to the phase speed of the wave causing the wave to break or saturate. In the winter months the wind speed doesn't change direction as you go up in altitude. In the summer months it changes direction as you go up in altitude and thus crosses the zero wind line.

In August 2009 the Andes Lidar Observatory (ALO), located close to the Cerro Pachon astronomical observatory in Chile (30.3°S, 70.7°W), started observations of the MLT region (see Figure 1). ALO was specifically designed to investigate the dynamics of the MLT using a suite of instruments including a Na wind-temperature lidar, a meteor-wind radar, an all-sky airglow imager and photometer suite, and a novel Mesospheric Temperature Mapper (MTM) camera developed at USU. The measurement of temperature is particularly important for understanding the dynamics of the MLT region. It provides information on the background structure of the atmosphere and the effects of wave perturbations. One of the longest and most established techniques for long-term measurements of mesospheric thermodynamics utilizes ground-based measurements of airglow emission rotational

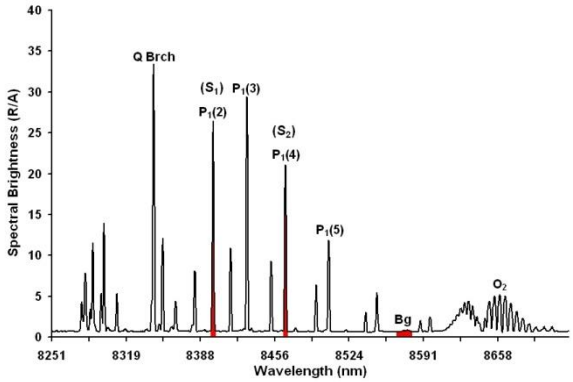


**Figure 3.** Emissions given by different OH vibrational mode transitions. The ratio of the $P_1(2)$ to $P_1(4)$ emissions (highlighted in red) is used to measure OH rotational temperature.

temperature. The most frequently used emissions are the near infrared OH Meinel bands and the $O_2$ (0,1) Atmospheric band.

## 2. BACKGROUND

### *2.1 Mesospheric Temperature Mapper*

The CEDAR mesospheric temperature mapper (MTM) is a high performance imaging system capable of precise measurement of the intensity and rotational temperatures of the near infrared OH nightglow emission layer which occur at peak altitude of ~87 km. The MTM uses a high quantum efficiency CCD array coupled to a wide-angle telecentric lens system (90° field of view centered on the zenith) to observe selected emission lines in the OH (6,2) Meinel band as shown in Figure 3. Sequential measurements were made using a set of narrow band filters centered on the OH $P_1(2)$ and $P_1(4)$ emission lines at 840 and 846.5 nm respectively. Each emission is observed for 30 sec followed by a background sky measurement at 857 nm, resulting in a cycle time of ~2 min. The camera operates automatically from dusk to dawn (for solar depression angles >12°) for approximately 23 nights each month (centered on the new moon period). Data are stored locally on computer disk and are downloaded at regular intervals to USU for analysis. To date, over 900 nights of quality

data have been obtained, providing detailed information on the nocturnal and seasonal behavior of mesospheric temperature and its variability at the OH emission height.

Relative intensity measurements of the selected OH emission lines are used to determine absolute rotational temperatures with high precision ~1-2 K using the well-established ratio method [eg. Meriwether, 1984, Goldman et al., 1998]. Based on typical OH emission levels measured at Cerro Pachon, the precision of the measurements were determined to be <1-2 K (in 3 min) for the derived OH rotational temperatures. A previous comparison of the MTM OH rotational temperature with other well calibrated instruments has shown that our nocturnal mean temperatures, referenced to 87 km, are accurate to ± 5K [Pendleton Jr., et al, 2000].

### *2.2. SABER*

NASA's spaceborne instrument called SABER (Sounding of the Atmosphere using Broadband Emission Radiometry) allows researchers to learn more about the upper atmosphere by helping produce the first comprehensive global measurements of this region. SABER, built by Utah State University's Space Dynamics Laboratory and managed by NASA Langley Research Center, is one of four instruments on the TIMED (Thermosphere, Ionosphere, Mesosphere, Energetics and Dynamics) spacecraft launched in late 2001. The technique that SABER uses to sound, or make measurements in the atmosphere, has never before been used to study the MLT region in such detail. SABER uses a 10-channel broadband limb-scanning infrared radiometer covering the spectral range from 1.27 μm to 17 μm. These limb scans view radiation emitted by the atmosphere such as in the form of airglow and provide vertical profile measurements of temperature, pressure, geopotiential height and chemical structures of the atmosphere between 10 and 180 km in altitude. The instrument provides fundamental information on the energy balance, chemistry, dynamics and transport of the MLT region [Russell III, et al., 1999].

## 3. DATA ANALYSIS

### *3.1. MTM Data*

The MTM data are stored as images and processed using software developed at USU. The background stars are first removed from the images. The intensity of the center pixels (zenith) of each of the $P_1(2)$, $P_1(4)$, background and dark images are next recorded. The OH rotational temperatures are derived as a function of time from these intensity measurements using the above mentioned ratio method.

This procedure is repeated for each clear, moonless night. The mean temperature values for each night are then recorded and plotted along with the standard deviation shown as the vertical error bars in Figure 4 in order to reveal the nightly variations for the entire run of data from August 12, 2009 until February 25, 2014. Each night the temperature variation can range from ± 5 K up to ± 20 K. A 15 night average smoothing curve is applied to the data; this is shown in Figure 4. Each year in the plot is separated by a vertical dashed line and average nightly OH rotational temperature for each is shown. The average OH temperature for the 54 months is 198 ± 9 K.

As mountain waves propagate upwards their amplitude grows which can be seen in the temperature measurements. The dominance of mountain wave activity in the winter months can be inferred by looking at the temperature variance ($\sigma^2$) as modeled by Jiang [Jiang, et al., 2002]. This is in agreement with results reported nearby at El Leoncito, Argentina [Reisin, Scheer, 2004]. In Figure 5a, temperature variances are

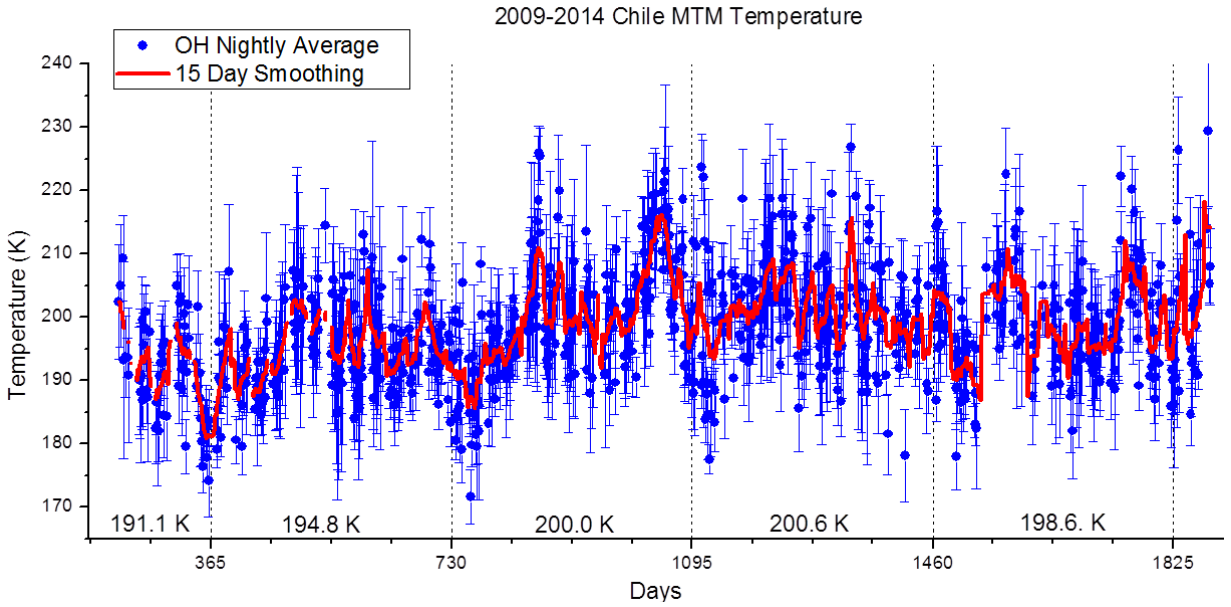


**Figure 4**. MTM nightly averaged OH temperature measurements from August 12, 2009 until Feb 25, 2014. Days are counted from January 1, 2009, where years are separated by black vertical lines. The blue points are the mean temperature for each night and the error bars represent the standard deviation in temperature each night. A 15-day running average smoothing fit (red line) is shown.

recorded for 4 years of data (1998-2002) for $O_2$ (solid line) and OH (dashed line) Rotational temperatures. In Figure 5b, the large-scale tidal features have been subtracted from the data. Similar results have also been found at ALO. In Figure 6 the tides (large-scale wave features) have not been removed, but Increased temperature variation during the winter months is still visible at ALO. Note the similarities of Figures 5a and 6.

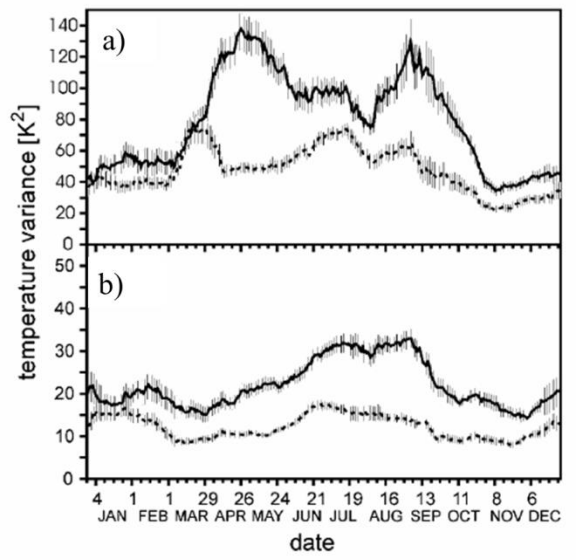


**Figure 5:** Plots of temperature variance from Reisin, Scheer, 2004 with a) tides included and b) tides removed. The solid line is for $O_2$ emissions (~93 km), the dashed line is OH (~87 km). Note both show increased temperature variation during the winter months and similarity to Figure 6.

### *3.2. SABER Comparison*

Once nocturnal OH temperature measurements are obtained by the MTM at ALO, a comparison with the SABER instrument can be made. As the TIMED satellite orbits earth SABER makes

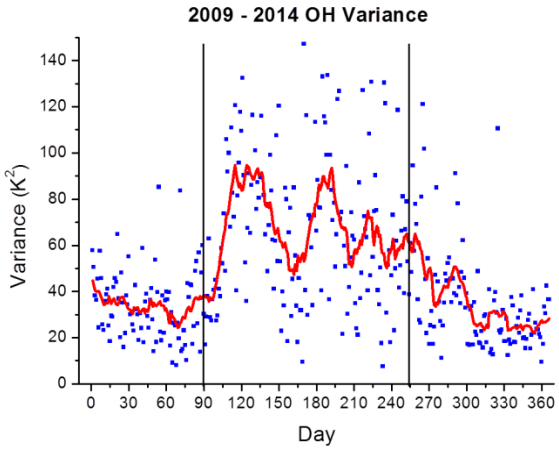


**Figure 6**. OH temperature variance for each night folded into one year (blue) with 30 day running average (red line) with tides still included, which increase variability. Enhanced variance is visible in the winter months (between two vertical black lines).

temperature profile (altitude ranges from ~15-110 km) measurements every ~30 sec as a unique event in numbered orbit. Along with the temperature profile SABER records the time and location. First, all events that are recorded at night within a 10° x 10° box centered at the ALO (30.3°S, 70.7°W) are selected by an IDL software program. The temperature is height weighted with a Gaussian profile in order to compare SABER and MTM OH temperatures at the nominal OH emission layer at 87 km. Often there will be two to four SABER events that will happen in the geographic box during one night. Each of the SABER temperature measurements is compared to the closest in time averaged MTM temperature measurement. All SABER events that are within 30 min coincident to MTM temperature measurements from August 2009 to February 2014 are plotted in Figure 7. The multiple years of data are folded into one year for viewing. SABER height weighted temperature measurements (green) average 192 ± 11 K and MTM OH temperature measurements (blue) average 198 ± 11 K for the 56 months of data. The averaged MTM OH temperature for each year is stable at around ~195 K while the SABER temperature had more variation year to year. The average offset in temperature of the two instruments was 6.0 ± 0.6 K.

### *3.3. Maui Comparison*

From November 2001 to December 2006 the MTM instrument suite operated from the Air Force AMOS facility near the summit of Haleakala Crater, Maui, Hawaii (altitude 2970 m, 20.8°N, 156.2° W) [Zhao et al., 2005]. Temperature comparisons with the MTM and SABER were conducted from Maui. The MTM in Maui had an average temperature of 202.2 K and SABER's average temperature was 197.0 K. They had a similar difference of 5.2 ± 0.2 K. What is of interest is the amount of variation that is apparent at ALO as opposed to Maui. The temperature difference between SABER and ALO measurements had a standard

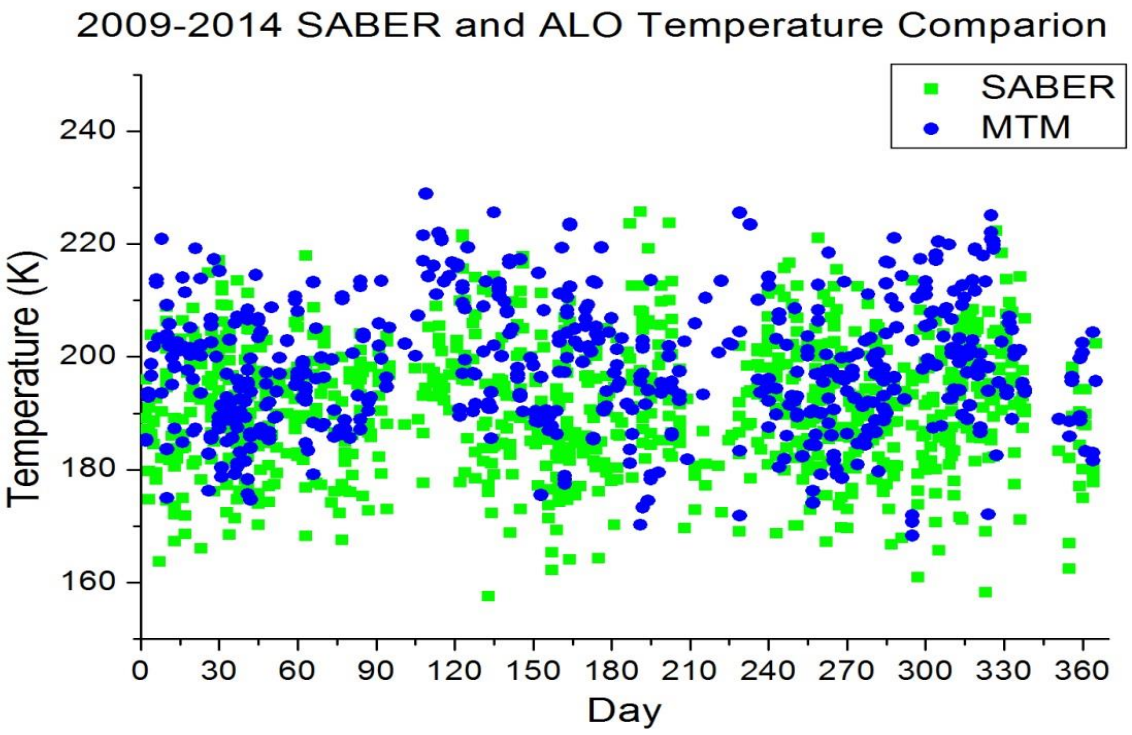


**Figure 7**. Coincident SABER temperature measurements and MTM OH temperature measurements for August 2009 to February 2014 folded into one year. SABER average temperature is 192 K and MTM OH average temperature is 198 K.

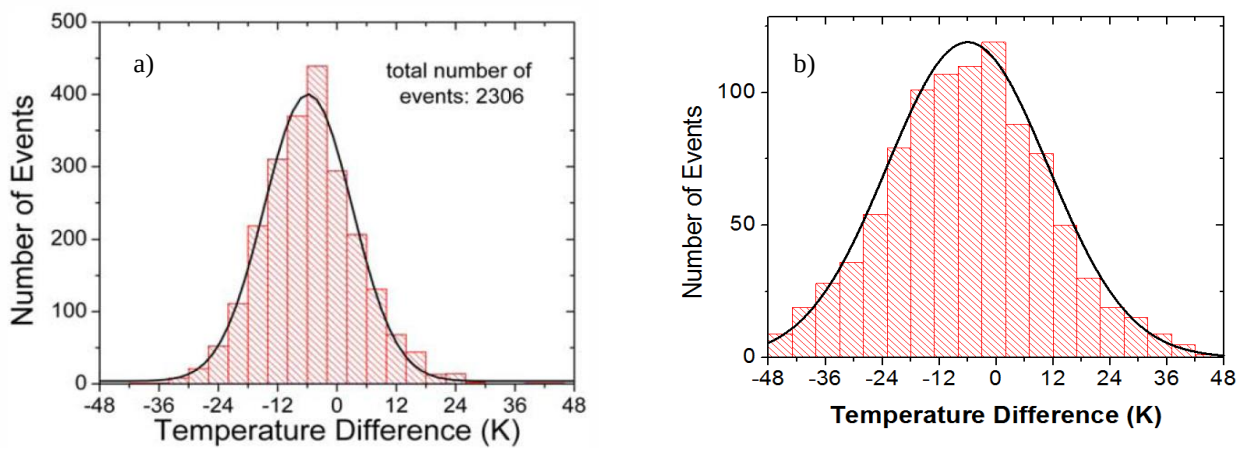


**Figure 8**. Histograms showing a) temperature difference between Maui and SABER and b) temperature difference between ALO and SABOR. Both show a temperature offset of ~5 K. Note that the FWHM is twice at ALO than Maui possibly revealing the increased mountain wave activity.

deviation of 16.9 K, where Maui's had a standard deviation 8.9 K. This may be due to the increased mountain wave activity observed at ALO. This is shown in the two histograms in Figure 8 with Gaussian fits. Further investigation of evidence of mountain wave activity is ongoing.

## 4. MCMURDO DATA

As part of a project to better understand AGW activity over Antarctica, Utah State University's Atmospheric Imaging Lab operates all-sky cameras and a MTM camera at several research stations around the perimeter of Antarctica and at the South Pole. One all-sky CCD camera at McMurdo Station (77°S, 166°E) on Ross Island off the coast of Antarctica. The all-sky camera at McMurdo has operated during the dark winter months from March to September for two years. Here is presented preliminary processed data from the 2012 season.

In the images recorded every ~10 seconds individual AGW events are observed in the OH emission layer. Using software developed at USU the horizontal wavelength and the direction of propagation of the waves are recorded. A total of 160 AGW events have been observed. The average

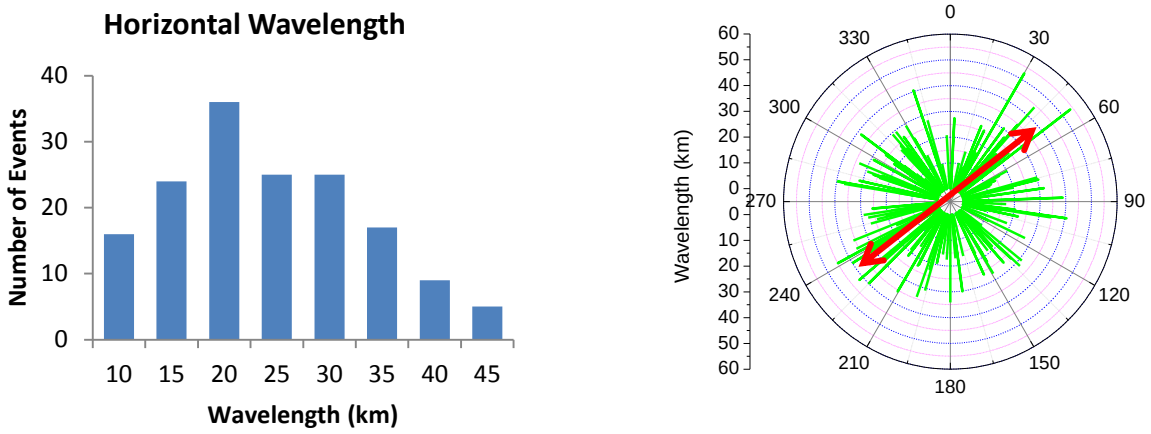


**Figure 9:** Histogram and polar plot summarizing McMurdo gravity wave measurements. Histogram on left shows distribution of horizontal wavelength of gravity waves observed at McMurdo during the 2012 season. On right, a polar plot oriented with North up at 0°shows the directionality of the gravity waves as a function of horizontal wavelength. Notice the apparent isotropy (preferred directions of propagation) highlighted by the red arrows.

horizontal wavelength of the AGW is 22 km and the direction of propagation reveals East-West direction dominance (shown in Figure 9). Note also the prevalence of long wavelength AGW to propagate North-eastward and South-westward as indicated by the arrow. This research is ongoing with more events needed to be processed in the 2012 season as well as the recent 2013 season.

## 5. CONCLUSION

Nocturnal variations of temperature at the ALO are highly variable and at times exceed 40 K during the course of the night probably driven by tidal oscillation (periods of 8 and 12 hours). Other nights show evidence of smaller amplitude gravity waves. Increased temperature variance in the winter months is a strong indication of the presence of mountain waves and is in agreement with models and other sites.

SABER temperature comparisons with ALO demonstrate the stability of ongoing MTM observations. These data are important for studying a broad range of wave phenomena extending from short period waves to seasonal variation. Comparisons with results from Maui show increased gravity wave activity over the Andes Mountains which with our variance measurements indicate that the prominent wave source is orographic forcing (created by mountains).

Optical observations of gravity wave activity over the Antarctic Continent is a new and ongoing study. Initial results are promising although further data reduction and analysis is needed.

Building on the results that temperature variances are a good indicator of increased mountain wave activity (see Figure 6) and seeing that temperature variability increases in regions with enhanced mountain wave activity (see figures 8) future research will focus on using SABOR data to measure temperature variances. Based on the method described in [Jiang, et al., 2002] measurements of temperature variance as a function of altitude will be used to investigate the growth of mountain wave amplitude, measure the characteristics of mountain waves and explore under what atmospheric conditions they break or saturate. Once the software is written, it can be used over at other locations for quantitative comparison of mountain wave activity. Further understanding of mountain waves will improve parameterization of waves in weather and turbulence forecast models.

**ACKNOWLEDGEMENTS.** I would like to thank my major professor Dr. Mike Taylor for his continued support. Also, this research could not be done without the help of Dr. Yucheng Zhao and Dr. Dominique Pautet. This research is supported under NSF grant #0737698.

**REFERENCES**

Eckerman, S.D. and P. Preusse (1999), Global Measurements of Stratospheric Mountain Waves from Space, *Science*, 286, 5444, 1534-1537.

Fritts, D.C., and M.J. Alexander (2003), Gravity wave dynamics and effects in the middle atmosphere. *Review of Geophysics*, 41, 1/1003.

Goldman, A., Schoenfeld, W.G., Goorvitch, D., Chackerian Jr., C., Dothe, H., Me1en, F., Abrams, M.C., Selby, J.E.A. (1998), Updated line parameters for the OH $X^2$ Π -$X^2$Π (v",v') transitions. J. Quant. Spectrosc. Radiat. Transfer, 59, 453-469.

Jiang, J. H., Wu, D. L., & Eckermann, S. D. (2002). Upper Atmosphere Research Satellite (UARS) MLS observation of mountain waves over the Andes.*Journal of Geophysical Research: Atmospheres (1984–2012)*, *107*(D20), SOL-15.

Meriwether, J.W. (1984), Ground based measurements of mesospheric temperatures by optical means. MAP Handbook 13, 1-18.

Pendleton Jr., W.R., Taylor, M.J., Gardner, L.C. (2000), Terdiurnal oscillations on OH Meinel rotational temperatures for fall conditions at northern mid-latitude sites. GRL 27 (12), 1799-1802.

Reisin, E. R., & Scheer, J. (2004), Gravity wave activity in the mesopause region from airglow measurements at El Leoncito. *Journal of Atmospheric and Solar-Terrestrial Physics, 66*(6), 655-661.

Remsberg, E. E., et al. (2008), Assessment of the quality of the Version 1.07 temperature-versus-pressure profiles of the middle atmosphere from TIMED/SABER, J. Geophys. Res., 113, D17101, doi:10.1029/2008JD010013.

Russell III, James M., et al. 1999, Overview of the SABER experiment and preliminary calibration results. *SPIE's International Symposium on Optical Science, Engineering, and Instrumentation*. International Society for Optics and Photonics Conference

Taori, A. and M.J. Taylor (2006), Characteristics of wave induced oscillations in mesospheric $O_2$ emission intensity and temperature, *Geophys. Res. Lett., 33*.

Zhao, Y., M. J. Taylor, and X. Chu (2005), Comparison of simultaneous Na lidar and mesospheric nightglow temperature measurements and the effects of tides on the emission layer heights, J. Geophys. Res., 110, D09S07, doi:10.1029/2004JD005115.

Zhao, Y., Taylor, M.J., Liu, H.-L., Roble, R.G. (2007), Seasonal oscillations in mesospheric temperatures at low-latitudes. JASTP 69, 2367-2378.